Development 135, 3113-3124 (2008) doi:10.1242/dev.022616

Single-cell gene profiling defines differential progenitor subclasses in mammalian neurogenesis

Ayano Kawaguchi[1,*], Tomoko Ikawa[1], Takeya Kasukawa[2], Hiroki R. Ueda[2,3], Kazuki Kurimoto[4], Mitinori Saitou[4] and Fumio Matsuzaki[1,5,*]

Cellular diversity of the brain is largely attributed to the spatial and temporal heterogeneity of progenitor cells. In mammalian cerebral development, it has been difficult to determine how heterogeneous the neural progenitor cells are, owing to dynamic changes in their nuclear position and gene expression. To address this issue, we systematically analyzed the cDNA profiles of a large number of single progenitor cells at the mid-embryonic stage in mouse. By cluster analysis and in situ hybridization, we have identified a set of genes that distinguishes between the apical and basal progenitors. Despite their relatively homogeneous global gene expression profiles, the apical progenitors exhibit highly variable expression patterns of Notch signaling components, raising the possibility that this causes the heterogeneous division patterns of these cells. Furthermore, we successfully captured the nascent state of basal progenitor cells. These cells are generated shortly after birth from the division of the apical progenitors, and show strong expression of the major Notch ligand delta-like 1, which soon fades away as the cells migrate in the ventricular zone. We also demonstrated that attenuation of Notch signals immediately induces differentiation of apical progenitors into nascent basal progenitors. Thus, a Notch-dependent feedback loop is likely to be in operation to maintain both progenitor populations.

KEY WORDS: Cortical development, Neurogenesis, Single-cell cDNA, Neural progenitors, Notch signaling

INTRODUCTION

During mammalian cerebral development, neural progenitor cells reside mainly in the ventricular zone (VZ) and the subventricular zone (SVZ). Neocortical progenitor cells are categorized into two distinct cell types based on their mitotic positions (Buchman and Tsai, 2007; Götz and Huttner, 2005; Kriegstein et al., 2006). The first type is the apical progenitor, which can function as a stem-like undifferentiated progenitor cell. These cells are essentially epithelial with a radial-glial-like morphology, and undergo interkinetic nuclear migration in the elongated cytoplasm and divide at the apical (ventricular) surface (Chenn and McConnell, 1995; Sauer and Walker, 1959; Takahashi et al., 1995). The second type is the basal progenitor (intermediate progenitor cell). These cells originate as daughters of the apical progenitors and migrate outward to the SVZ, where they undergo terminal mitosis and generate a pair of neurons at the mid-embryonic stage (Haubensak et al., 2004; Miyata et al., 2004; Noctor et al., 2004).

Although the apical and basal progenitors can be distinguished from each other by several molecular markers and by their mitotic positions (Englund et al., 2005), the mechanism by which apical progenitors differentiate into basal progenitors and how their populations are controlled during cortical development are unclear. Furthermore, it is not clear whether the apical progenitor cells are composed of distinct populations. Some apical progenitors divide symmetrically, generating two daughters of the same type, but they are also capable of dividing asymmetrically to generate a single neuron and a progenitor cell, or two different types of progenitor cells (Guillemot, 2005; Huttner and Kosodo, 2005). This heterogeneity in division patterns may depend on differential properties among the apical progenitor cells. Molecular perspectives on progenitor heterogeneity (e.g. Gal et al., 2006; Hartfuss et al., 2001) are, thus, essential for studying these fundamental questions regarding neocortical development. However, the highly dynamic migratory behavior of neuronal progenitors during their cell cycle, in addition to possible temporal changes in their gene expression, have made it difficult to approach these issues.

The molecular framework behind the differentiation of progenitors into neurons relies on Notch signaling (Guillemot, 2005; Yoon and Gaiano, 2005). Although the neural cells expressing Notch ligands, such as Delta [delta-like 1 (Dll1) in mouse], have not been explicitly identified, they are thought to be differentiating neurons. In neural stem cells, activation of the Notch signal induces the bHLH transcription factors, Hes1 and/or Hes5, which in turn repress the expression of proneural genes such as neurogenin 2 (*Neurog2*), *NeuroD* (*Neurod1*) and *Ascl1* (*Mash1*). Proneural genes are transiently expressed in differentiating neurons, and induce expression of a wide spectrum of neuron-specific genes to promote neuronal differentiation. The role of Notch signaling in creating progenitor diversity, however, remains elusive in mammalian neurogenesis.

Here we analyzed the gene expression profiles (Tietjen et al., 2003) of a large number of single, isolated neocortical progenitor cells at the mid-embryonic stage to explore the diversity of neural progenitor cells. We manually picked up single cerebral cells without recourse to a cell sorter. By doing so, we minimized the time needed for single-cell isolation, and thereby also minimized the changes that occur in mRNA expression in cells during the isolation process. Furthermore, an improved single-cell cDNA amplification method (Kurimoto et al., 2006; Kurimoto et al., 2007) enabled us to perform quantitative high-density

[1]Laboratory for Cell Asymmetry, [2]Functional Genomics Unit, [3]Laboratory for Systems Biology and [4]Laboratory for Mammalian Germ Cell Biology, Center for Developmental Biology, RIKEN Kobe Institute, 2-2-3 Minatojima-minamimachi, Chuo-ku, Kobe, Hyogo 650-0047, Japan. [5]CREST, Japan Science and Technology Agency.

*Authors for correspondence (e-mails: akawa@cdb.riken.jp; fumio@cdb.riken.jp)

Accepted 28 July 2008

oligonucleotide microarray analyses of cDNA from individual cells and to investigate the heterogeneity of progenitors at the single-cell level.

MATERIALS AND METHODS

Animals

All animal experiments were performed in accordance with institutional guidelines. To time pregnant mice, the date the vaginal plug was observed was defined as embryonic day (E) 0.

cDNA synthesis from single cerebral cells

Small VZ/SVZ fragments or cortical plate (CP) fragments of the dorsolateral portion of a CD1 mouse cerebral wall at E14 were digested in 100 μl PBS containing 0.25% trypsin and 0.5% glucose for 5 minutes at 37°C and triturated. After adding Hank's solution (Nacalai, Japan) with trypsin inhibitor (Ovomucoid, Sigma), single, isolated cells were randomly picked up manually by glass capillary under an inverted microscope and transferred to PCR tubes containing 4.5 μl of cell lysis buffer spiked with RNA: poly(A)-tailed *Bacillus subtilis lys*, *dap*, *phe* and *thr* RNAs at 1000, 100, 20 and 5 copies per cell, respectively. cDNA synthesis after cell lysis was performed as previously described (Kurimoto et al., 2006; Kurimoto et al., 2007). The quality of the amplified cDNA samples was screened by the consistent amplification of the added RNAs and housekeeping genes [*Gapdh*, beta-actin (*Actb*), *Aldoa* and *Pabpn1*] by quantitative real-time PCR (Q-PCR) (the first quality check). cDNAs were subjected to another amplification step with primers bearing the T7 promoter sequence. The quality of these second PCR products was again examined by Q-PCR for housekeeping genes and the added RNA (the second quality check). In the case of the single-cell cDNAs of the progenitor cells, all samples that passed the secondary quality check were used for the GeneChip analysis.

Q-PCR analysis

Q-PCR was performed (primers as listed in Table 1) against the cDNAs before adding the T7 promoter sequence (the first quality check and examination of marker gene expression; see Table 2 and see Fig. S1 in the supplementary material), and against the second PCR products (the second quality check), using the 7900 Real-Time PCR system (Applied Biosystems) according to the manufacturer's instructions.

Microarray hybridization and data processing

cDNA samples were subjected to the One-Cycle Target Labeling procedure for biotin labeling by in vitro transcription (Affymetrix, Santa Clara, CA). The cRNA was subsequently fragmented and hybridized to the GeneChip Mouse Genome 430 2.0 array (Affymetrix), according to the manufacturer's instructions. The microarray image data were processed with a GeneChip Scanner 3000 (Affymetrix) and then analyzed using the Affymetrix Microarray Software 5.0 (MAS5.0) algorithm, and quantile normalization. A total of 76 cDNA samples were subjected to the GeneChip analysis, and after checking the data by a histogram of the expression values, qcAffy (Affymetrix), RNA degradation and RLE/NUSE (affyPLM) (the third quality check), 70 samples were used for further analysis. The linearity between the signal intensity and copy number of the original RNAs was monitored by the expression levels of the amplified added RNAs, and the signal intensity of the added RNAs at >20 copies per cell was proportional to the copy number (see Fig. S2 in the supplementary material), as reported (Kurimoto et al., 2006).

Data analysis

To identify significantly differentially expressed probe sets across Groups A, B and C (SigABC genes), the GeneChip data were subjected to analysis of variance (ANOVA) (Group A, n=7 samples; Group B, n=15; Group C, n=7) against each probe set on the GeneChip (n=45,037 probe sets). The false discovery rate (FDR) was calculated from the P-values of the ANOVA, and probe sets showing FDR<0.1 were selected as significantly different probe sets (n=114 probe sets) (see Table S1 in the supplementary material). The 'Over-20 copies' probe sets (n=10,493 probe sets) were defined as the probe sets for which at least 1 of 70 samples expressed >20 copies per cell, which was more than the signal level of 909.6 (the median expression level of 'AFFX-PheX-3_at', the probe set for the spiked RNA *phe*, 20 copies per sample). Since RNAs spiked at 20 copies per cell or more were consistently and proportionally amplified by our method (see Fig. S2 in the supplementary material), we used these Over-20 copies probe sets for the unsupervised clustering analysis. Cluster analysis of the 70 samples was performed using

Table 1. Gene-specific primers used for Q-PCR of single-cell cDNA

Gene	5′ primer (5′ to 3′)	3′ primer (5′ to 3′)
Bacillus lys	GCCATATCGGCTCGCAAATC	AACGAATGCCGAAACCTCCTC
Bacillus dap	CCAGACCGCGGCCTAATAATG	CGCTTCTTCCACCAGTGCAG
Bacillus phe	TGAGCTCTAGGCCCAAAACGAC	TCCGGTTTTAGTCGGACGTG
Bacillus thr	GCCGATGCCGTAAAAGCAAG	CAGCTCAGGCACAAGCATCG
Gapdh	ATGAATACGGCTACAGCAACAGG	CTCTTGCTCAGTGTCCTTGCTG
Aldoa	TTCAGGCTCTTTCCCATCACTCTTGC	AGCATTCACAGACAACACCGCACACG
beta actin	CAGCAAGCAGGAGTACGATGAGTC	CAGTAACAGTCCGCCTAGAAGCAC
Pabpn1	ACCAGGCATCAGCACAACAGACCG	CCACTGTAGAATCGAGATCGGGAGCTG
Ki67 (*Mki67*)	GCTTTGAGCTTTCCTGGTCATACTC	GCTTTATTGGATAGGACAGAGGGC
p57 (*Cdkn1c*)	CAGAGAGAACTTGCTGGGCATC	CGGTTCCTGCTACATGAACGAAAG
cyclin E1 (*Ccne1*)	TGAGTGCTCCAGAAGCTGCTAAGG	TGTCATCTGTGTGAAGAGTCCAGTG
cyclin B1 (*Ccnb1*)	TGCCCTCCACAGTGTTCTTAAATG	AGCACCCCCTGGAAGACTACTATG
Hes1	TCCTAACGCAGTGTCACCTTCCAG	CCAAGTTCGTTTTTAGTGTCCGTC
Hes5	TTCCTTTGTATGGGTGGGTGC	GAAGCCTTCAGAACAGCCTGTG
Pax6	ACAACACAGGCTGTTGGATCGC	GGCAAATCTTGTCGATCATGGTTTCC
Notch1	AGGACTGTCAGACTGTGGCTTAGC	ATCCTGGGTTGTGCTCTTAGGAG
Otx1	TGAACCTTCCTTCTCCGAAATCTGC	ACTTTCCCACCTACTGAACCAAGCG
Sox2	CATGAGAGCAAGTACTGGCAAG	CCAACGATATCAACCTGCATGG
Neurog2	GTCAAAGAGGACTATGGCGTGTG	TACAGTCTTACGAGGTTCCCCACG
HuB (*Elavl2*)	GGTTTCATTTTCGTAATCACCAGTGGG	GCCATCTATCACATAACAACCAGGATG
Epha3	AGCCAAGTGCCAAATGCTATTG	GGTGACAGTAGGAACAGGGAAAGC
Svet1	CCTCACCCTTTACCTGTAAGTAGCC	GCAAGGATACCAGCAAAACCCTAC
Tbr2	CAAAGGCATGGGGGCTTATTATGC	CAAAACACCACCAGGTCCATCTGG
Cxcl12	CCCAAAACCCACTCAGCAAAG	ATAGGAAGCTGCCTTCTCCTGGAC
Dll1	AAGGATATAGCCCCGATGAATGC	TGCTAACTCTGAGAGAACCAGCTTCG
Tis21 (*Btg2*)	GGTTGGAGAAAATTGGGAAACACTGG	GCTCTAGCTCTGTCCTTCAGTTTGAGAGAC
Cux2	AGCGGCGGCATGAGAAAATG	AATTCCCACTCCAGGACCTCTTC
Dlx1	AAGCACCCCAATTCCAGGTC	GATGACTTGTGTTCTGTGGTCGAG

the GeneChip data of the SigABC genes (Fig. 1A) or of the Over-20 copies probe sets (Fig. 1B). Hierarchical clustering with approximately unbiased (AU) *P*-values, computed by multiscale bootstrap resampling for assessing the uncertainty in the hierarchical cluster analysis, was performed using the R software package pvclust (Suzuki and Shimodaira, 2006), with nboot=10,000, distance correlation and complete-linkage cluster analysis.

The probe sets with significantly different expression between Cluster I and II/III (n=1440 probe sets, FDR<0.1) were identified by Welch's t-test, and between Cluster I (n=33 samples) and II/III (n=23) against each Over-20 copies probe set (n=10,493 probe sets) and FDR were calculated from the two-tailed *P*-values using the R software package Q-value (http://genomics.princeton.edu/storeylab/qvalue). Among these significant probe sets (n=1440 probe sets), the top 175 Cluster I genes (log fold-change cut-off <–2.50) and the top 117 Cluster II/III genes (log fold-change cut-off >2.50) were further used for the hierarchical cluster analysis shown in Figs 2 and 4. The value of the log fold-change was obtained by subtracting the mean of logarithmic signal values in Cluster I cells from the mean of logarithmic signal values in Cluster II and III cells.

The probe sets that were significantly differentially expressed between Cluster I and Cluster II/III (n=1440 probe sets) were further analyzed for their functions using Ingenuity Pathway Analysis [(IPA) Ingenuity Systems, Redwood City, CA]. Among the 1440 probe sets, 1400 genes were mapped and 576 were matched in the pathway of the IPA database. These 576 genes were used to look for significant differences among the canonical signaling pathways by IPA.

RNA in situ hybridization

Non-radioactive in situ hybridization of frozen sections of E14 CD1 mouse brain or cultured slices was performed using antisense RNA probes (see Table S2 in the supplementary material) labeled with digoxigenin (DIG) (Roche, Basel, Switzerland). In some cases, in situ hybridization data were obtained from a website database (GenePaint; http://www.genepaint.org), and in these cases the GenePaint set ID is indicated in the figure (Fig. 3, Fig. 4B).

Slice culture with DAPT treatment

Coronal slices of dorsolateral forebrain were prepared from E14 CD1 mice as previously described (Miyata et al., 2004), and cultured in collagen gel in growth medium [DMEM/F12 with B27 (Gibco), N2 (Gibco), 5% FBS, 5% horse serum, 10 ng/ml Fgf2 and 20 ng/ml Egf] with 10 μM DAPT {γ-secretase inhibitor *N*-[N-(3,5-difluorophenacetyl)-L-alanyl]-S-phenylglycine t-butyl ester} (Sigma) or an equal volume of DMSO (Nacalai), at 36°C with 5% CO_2 and 30% O_2. After 7 or 20 hours, the slices were fixed in 4% PFA in PBS and used for immunohistochemistry or in situ hybridization as cryosections.

Immunochemistry

Antibodies used for the immunostaining of cryostat sections or fixed cells were: anti-BrdU (mouse IgG, Roche; rat IgG, Abcam), anti-GFP (chick, Aves Labs), anti-cyclin A (rabbit, Santa Cruz), anti-Ki67 (mouse IgG, BD Biosciences; mouse IgG, Novocastra), anti-Tbr2 (rabbit, Abcam), anti-Dll1 (sheep IgG, R&D Systems), anti-PH3 (mouse IgG, Sigma), anti-Vcam1 (rat IgG, BD Pharmingen) and anti-cleaved caspase 3 (rabbit, Cell Signaling). In some cases, the primary antibody was labeled with Alexa488 (Zenon Alexa Fluor Labeling Kit, Molecular Probes) prior to use. Secondary antibodies were conjugated to Alexa488 or Alexa568 (Molecular Probes), Cy3 or Cy5 (Jackson). Nuclei were counterstained with DAPI.

Microarray data

Microarray data are available on the GEO database with accession number GSE10881.

RESULTS

Typical and atypical cortical progenitor cells for marker gene expression

We randomly picked up single cells from the VZ/SVZ of E14 mouse dorsal forebrain, and a total of 102 single-cell cDNA samples, including nine derived from the CP to obtain information from mature neurons, were amplified as described (Kurimoto et al., 2006; Kurimoto et al., 2007) (Table 2).

Stem-like cells, i.e. undifferentiated neural progenitor cells in the VZ, are considered to express Hes1 and not Neurog2 (Yoon and Gaiano, 2005). Cells that express high levels of Neurog2 in the VZ are thought to be progenitors that are biased toward neuronal production (Britz et al., 2006), whereas mature basal progenitors are expected to express SVZ regional markers such as *Svet1*

Table 2. Neural progenitor cells categorized by region and differentiation markers

Cell type	*n*	*n* for GeneChip
***Svet1*⁻ progenitor (VZ progenitor)**		
Hes1⁺/*Neurog2*⁻	8 (=Group A)	7
Hes1⁺/*Neurog2*⁺*	17	15
Hes1⁻/*Neurog2*⁺	17 (=Group B)	15
Hes1⁻/*Neurog2*⁻	9	7
***Svet1*⁺ progenitor (SVZ progenitor)**		
Hes1⁻/*HuB*⁺ or *Epha3*⁺ (typical SVZ progenitor)	10 (=Group C)	7
Hes1⁻/*HuB*⁻/*Epha3*⁻	1	1
Hes1⁺	5	4
***Svet1*⁺ neuron**		
HuB⁺ or *Epha3*⁺/*Pax6*⁻/*Neurog2*⁻/*Sox2*⁻ (typical SVZ neuron)	12 (=Group D)	7
Pax6⁺ or *Neurog2*⁺ or *Sox2*⁺ (their expression was weak if any)	6	3
***Svet1*⁻ neuron**		
HuB⁺ or *Epha3*⁺	7	
CP neuron‡	9 (=Group E)	3
Other		
Tangential migrating progenitor cells, *Dlx1*⁺	1	1
Total	102	70

A total of 102 single-cell cDNAs were obtained from the mouse E14 cerebral wall and were categorized into five groups (A-E) based on their expression of marker genes (see Fig. S1 in the supplementary material) as determined by Q-PCR, including cell-cycle-related genes (*Ki67*, cyclin B1, cyclin E1), SVZ regional markers [*Svet1*, *HuB* (*Elavl2*), *Epha3*] and differentiation-related genes (*Hes1*, *Neurog2*, *Sox2*, *Pax6*). A total of 76 samples were subjected to DNA microarray analysis. After a quality check of the microarray data, 70 samples (shown in the right-hand column) were used for further analyses.

*These included seven samples that were *Neurog2*-negative by Q-PCR of the first PCR products, but positive in the GeneChip data of the second PCR products.

‡These cells were derived from the CP fragments of the cerebral wall, and the others were from the VZ/SVZ fragments.

(Tarabykin et al., 2001), because they exit the VZ to divide into neurons in the SVZ. Thus, as the first step in defining the subclasses of progenitor cells, we examined whether the single-cell cDNAs derived from these 'typical' progenitor cells could be identified in our cDNA samples. We subjected a portion of the samples to quantitative real-time PCR (Q-PCR), to examine the expression levels of twenty marker genes representative of the different cell states (Tables 1, 2; see Fig. S1 in the supplementary material).

In the Q-PCR analysis, we successfully identified cells that showed typical marker gene expression, and classified many of them into five groups (Groups A to E; Table 2). Group A cells were *Hes1*$^{+}$ *Neurog2*$^{-}$ *Svet1*$^{-}$, and represented typical undifferentiated progenitor cells in the VZ. Group B cells were *Hes1*$^{-}$ *Neurog2*$^{+}$ *Svet1*$^{-}$, and seemed to be neuronally biased progenitors in the VZ. Group C cells were *Svet1*$^{+}$ SVZ cells, presumably the basal progenitors. Group D cells were *Svet1*$^{+}$ young neurons, whereas Group E cells were mature neurons from the CP. However, many samples had other expression profiles and could not be assigned to these five groups; we named them 'Group X' cells.

We next subjected the same cDNA samples from all the progenitor groups (Groups A, B, C and X) and from the Group D and E cells to a second amplification step, and applied them to DNA microarrays (GeneChip, Affymetrix) to obtain their genome-wide gene expression profiles. After checking the quality of the microarray data, the results from 70 samples (70 microarrays; Table 2) were used for further examination.

Two distinct neural progenitor populations revealed by genome-wide gene expression profiles: Cluster I and Cluster II/III

To examine whether the neural progenitor cells, including the atypical Group X cells, could be classified according to their gene expression profiles, we performed hierarchical clustering of the 70 samples based on the microarray data (Fig. 1A,B).

First, we selected the set of genes that were differently expressed across typical progenitor groups [Groups A, B, C; named SigABC genes, n=114 probe sets, ANOVA, false discovery rate (FDR) <0.1; see Table S1 in the supplementary material], and performed a cluster analysis of the 70 samples using these probe sets (supervised clustering) (Fig. 1A). The four 'clusters', Clusters I to IV, were defined essentially based on this dendrogram. Cluster I included all Group A cells (putative undifferentiated progenitor cells) and most of the atypical Group X cells, many of which were *Hes1*$^{+}$ *Neurog2*$^{+}$ VZ progenitor cells (Table 2). Cluster II cells were mostly Group B cells, which were *Hes1*$^{-}$ *Neurog2*$^{+}$ VZ progenitor cells, whereas Cluster III comprised Group C cells (*Svet1*$^{+}$ basal progenitors). Cluster IV cells were neurons.

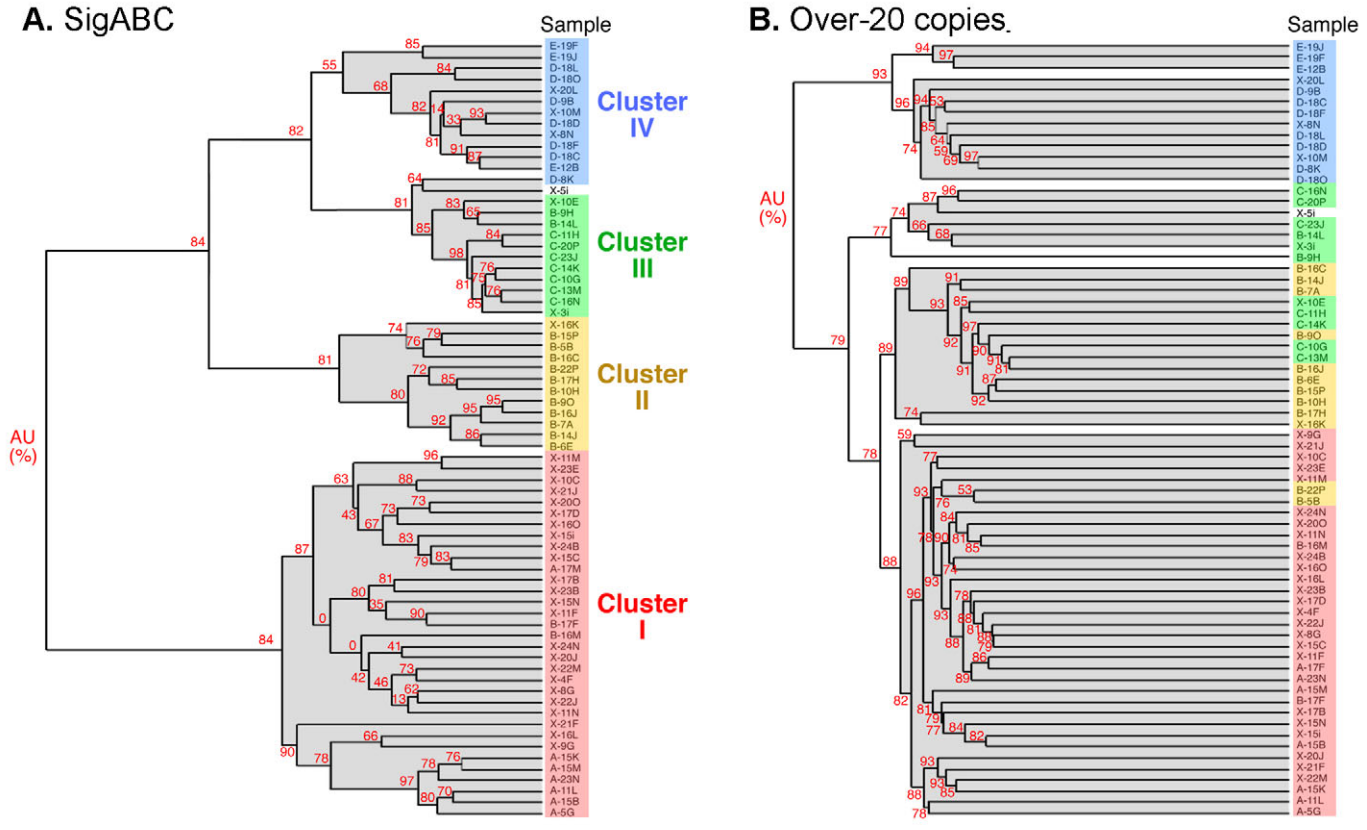

Fig. 1. Hierarchical clustering of single-cell cDNAs and definition of clusters. Cluster dendrograms showing the results from (**A**) SigABC genes (probe sets significantly different across Groups A, B and C; n=114 probe sets; see Table S1 in the supplementary material) and (**B**) 'Over-20 copies' probe sets (probe sets for which at least one of the 70 cDNA samples showed an expression level of >20 copies per cell; n=10493 probe sets). The dendrogram in A defines four clusters. In both dendrograms, each sample name represents one cell, and its color indicates the cluster to which it belongs. The first letter of the name indicates the cell group; for example, A-11L is a Group A cell. The values in red at the branches are AU (approximately unbiased) *P*-values (%) that indicate how strongly the cluster is supported by the data. For example, for a cluster with an AU *P*-value >95%, the hypothesis that 'the cluster does not exist' is rejected with a significance level of 5%. The horizontal branch length represents the degree of dissimilarity in gene expression among the samples.

In the hierarchical clustering diagram (Fig. 1A), the neural progenitor cells are roughly separated into two distinct populations comprising Cluster I and Cluster II plus III (Cluster II/III). Cluster II/III cells were closest to the Cluster IV neurons, occupying the same large branch, indicating that among the progenitor cells, the Cluster III cells were most closely related to neurons. Cluster I cells, including all the Group A cells, were more distant from neurons than were Cluster II cells, reinforcing our assumption that the VZ progenitor cells in Group A were more undifferentiated than those in Group B.

Since this cluster analysis included information from the categorization determined by Q-PCR, it was 'supervised' by information regarding the position and differentiation of progenitor cells, which we provided. We therefore performed an unsupervised cluster analysis of the 70 samples, in which the clustering was based only on the GeneChip data (Fig. 1B). In this case, we used all the probe sets that seemed to function in our experiments ('Over-20 copies' probe sets, *n*=10493, see Materials and methods). The large number of housekeeping genes among the probe sets and the huge dimensions (the probe set number) in the cluster analysis reduced the outcome difference among the samples (represented by the difference in the horizontal branch length in Fig. 1). Nonetheless, the unbiased clustering yielded essentially the same results as the supervised clustering. As shown in Fig. 1B, the 70 samples were divided into the two populations of neurons and progenitor cells, and the progenitor cell clusters largely corresponded to those defined by the SigABC conditions (Fig. 1A). This result further supported the division of neural progenitor cells into two distinct populations: Cluster I and Cluster II/III.

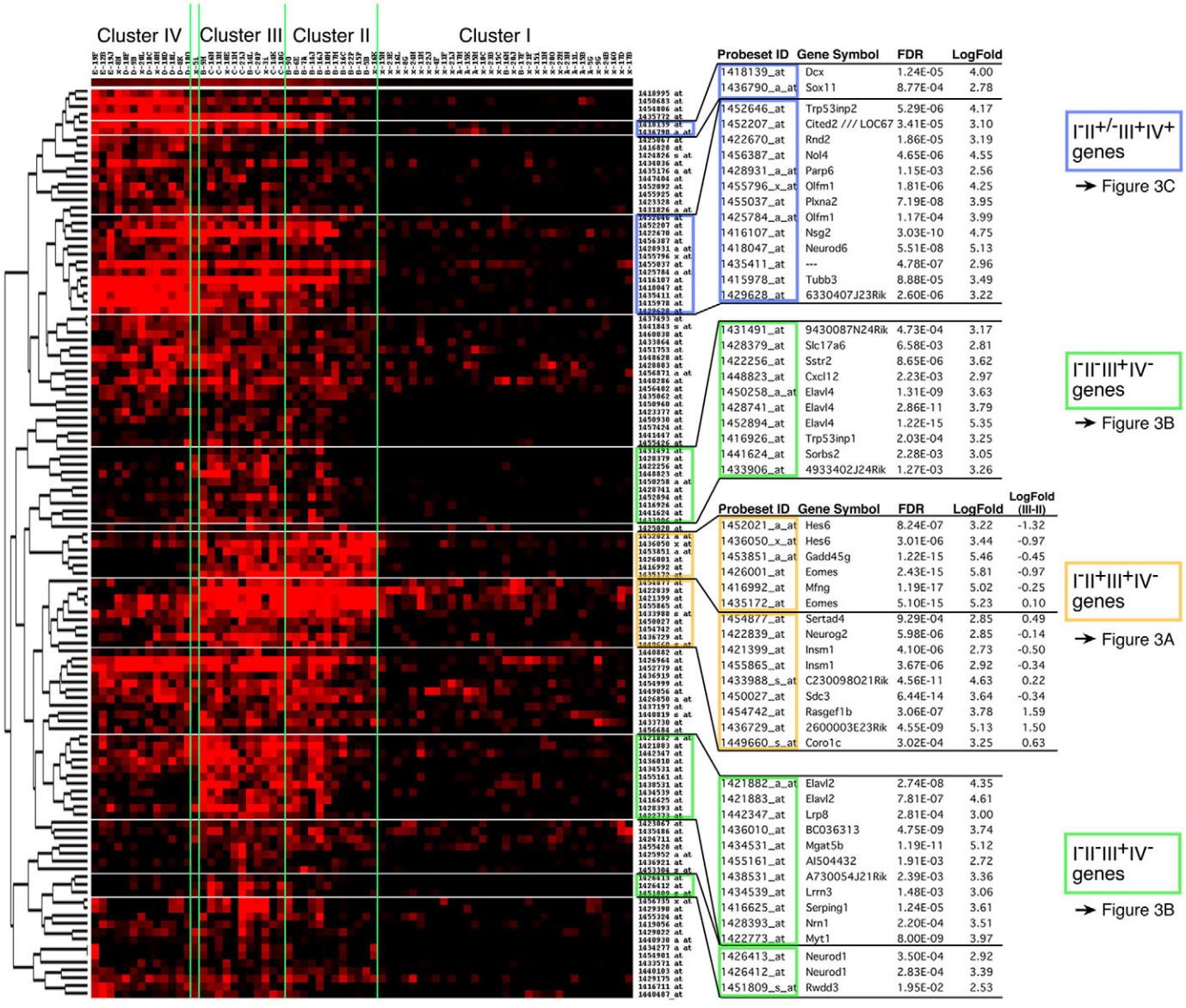

Fig. 2. Expression levels of Cluster II/III genes in single-cell cDNAs. Data from the probe sets that were expressed in Cluster II/III, but not in Cluster I, were used for clustering (*n*=117 probe sets; Welch's *t*-test, FDR<0.1, log fold-change cut-off >2.5). Each column indicates one cell, and each row indicates one probe set on the microarray. The expression levels are color-coded from red (high) to black (low). These probe sets were categorized into several groups based on their expression pattern along the clusters: probe sets that showed a typical expression pattern are grouped by color (blue, green or yellow). The in situ hybridization patterns of these genes are shown in Fig. 3. For the I^{-} II^{+} III^{+} IV^{-} genes (yellow), the log fold-changes from Cluster II to Cluster III cells are also indicated.

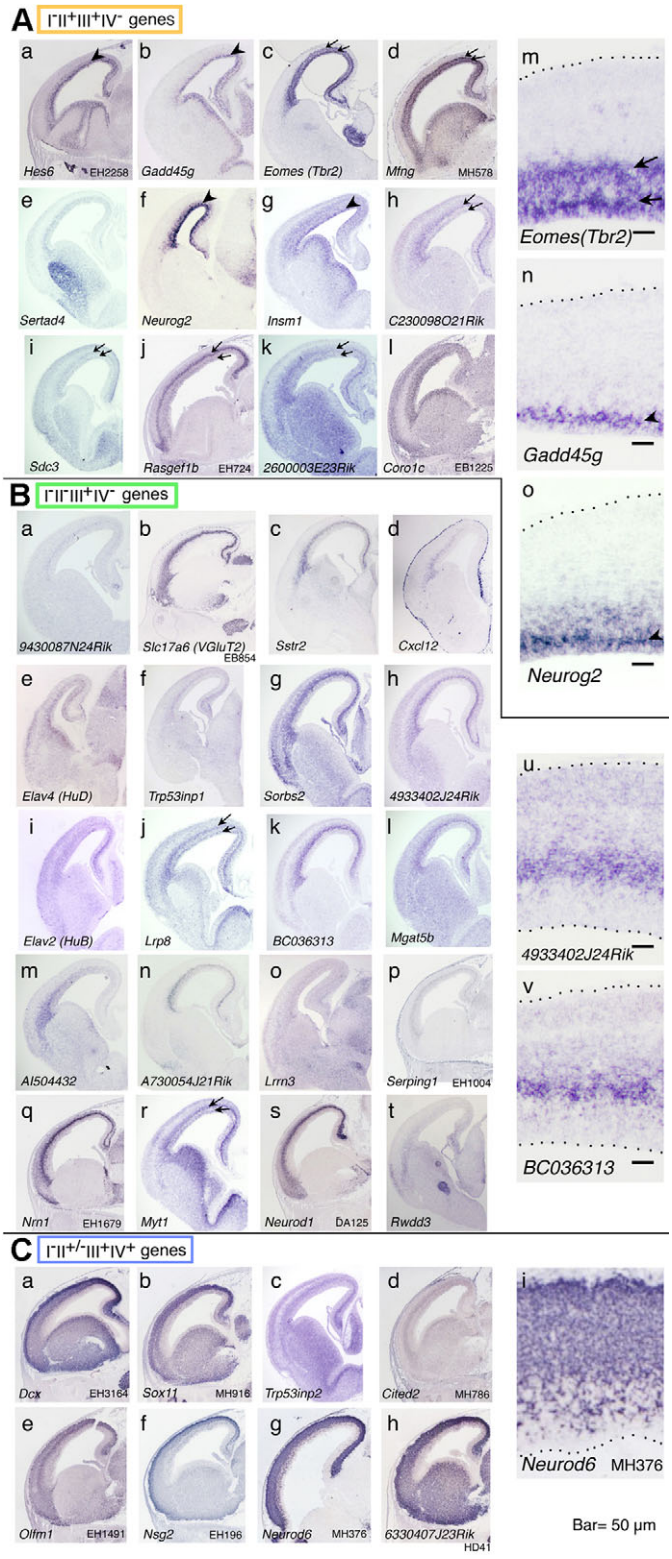

Fig. 3. mRNA expression of Cluster II/III genes in the E14 mouse brain. In situ hybridization of all of the (**A**) yellow (I^- II^+ III^+ IV^-) and (**B**) green (I^- II^- III^+ IV^-) genes, and some of the (**C**) blue (I^- $II^{+/-}$ III^+ IV^+) genes from Fig. 2. Magnified views of Ac,b,f are shown in Am,n,o, respectively; Bu,v show magnified views of Bh,k, respectively; Ci shows a magnified view of Cg. Signals for the I^- II^+ III^+ IV^- genes typically exhibited a two-band pattern in the SVZ and part of the VZ (arrows, Ac,d,h,i,j,k,m; see also Bj,r). For some genes, the band in the VZ was dominant (arrowhead, Aa,b,f,g,n,o). In both cases, the VZ signals were 20-40 µm from the apical surface (dotted line). GenePaint set IDs are indicated at the bottom right of some panels. Scale bars: 50 µm.

Genes representing each cluster show characteristic spatial expression patterns in vivo

To verify the cell-clustering results, we assessed whether the gene expression profiles that represented each cluster reflected the situation in vivo. For this purpose, we selected a set of genes that represented each cluster. When we compared Clusters I and II/III, 1440 among the Over-20 copies probe sets (n=10493) showed a significant difference in expression level (Welch's t-test, FDR<0.1). Of these, 175 were selected as Cluster I genes (log fold-change cut-off <–2.50), and 117 as Cluster II/III genes (log fold-change cut-off >2.50). The microarray data for these gene sets were used for cluster analysis to see whether these genes are further characterized by a dependency of their expression profiles on the four clusters of cells.

First, we focused on the Cluster II/III genes. This class included many neuronal genes (Fig. 2), suggesting that Cluster II and/or III cells are biased towards the neuronal fate. These genes were clustered according to their signal levels in the 70 individual cells from which the cDNAs were isolated. In these gene clusters, three characteristic patterns of gene expression emerged by aligning cells from Clusters I to IV (Fig. 2): (1) some Cluster II/III genes were mainly expressed in Clusters II and III (I^- II^+ III^+ IV^- genes); (2) some were mainly expressed in Cluster III (I^- II^- III^+ IV^- genes); and (3) some were mainly expressed in Cluster II (weakly in some cases), III and IV (I^- $II^{+/-}$ III^+ IV^+ genes). Notably, we could not find probe sets that were expressed only in Cluster II cells, but some of the probe sets for the I^- II^+ III^+ IV^- genes showed stronger signals in Cluster II than in Cluster III (for example, the probe sets for *Hes6* and *Gadd45g*).

We next examined the mRNA expression of these genes in E14 mouse brain and compared it with the gene profiling patterns. In situ hybridization revealed their expression in characteristic spatial patterns along the radial axis, which correlated with their expression in the clusters (Fig. 3A-C). The in situ hybridization signals for the I^- II^+ III^+ IV^- genes was typically split into two separate bands, an upper one in the SVZ and a lower one in a subdomain of the VZ, ~20-40 µm away from the apical surface (Fig. 3Ac,d,h-k,m). For some genes that showed a stronger signal in Cluster II than Cluster III, the lower band was dominant and the upper one was weak or undetectable (Fig. 3Aa,b,f,g,n,o). By contrast, the in situ hybridization signals for the I^- II^- III^+ IV^- genes were usually confined to the SVZ (Fig. 3B), consistent with the Cluster III cells being SVZ basal progenitor cells (Table 2 and Fig. 1). The genes categorized as I^- $II^{+/-}$ III^+ IV^+ showed signals in the SVZ and the intermediate zone (IMZ) or CP, where neurons exist (Fig. 3C). This was consistent with the Cluster IV cells being neurons.

These results demonstrated that the cell-clustering results based on gene profiling correlated well with the in situ hybridization patterns of the Cluster II/III genes, leading us to conclude that the signals in the lower band in the VZ originated from Cluster II cells, whereas the SVZ signals corresponded to Cluster III cells (the SVZ basal progenitor cells). The Cluster II and Cluster III cells thus share common features in both global gene expression and the in vivo expression of particular genes, although they are assigned to different regions along the radial axis of the brain. The basal progenitor (Cluster III) cells are born at the ventricular surface and migrate

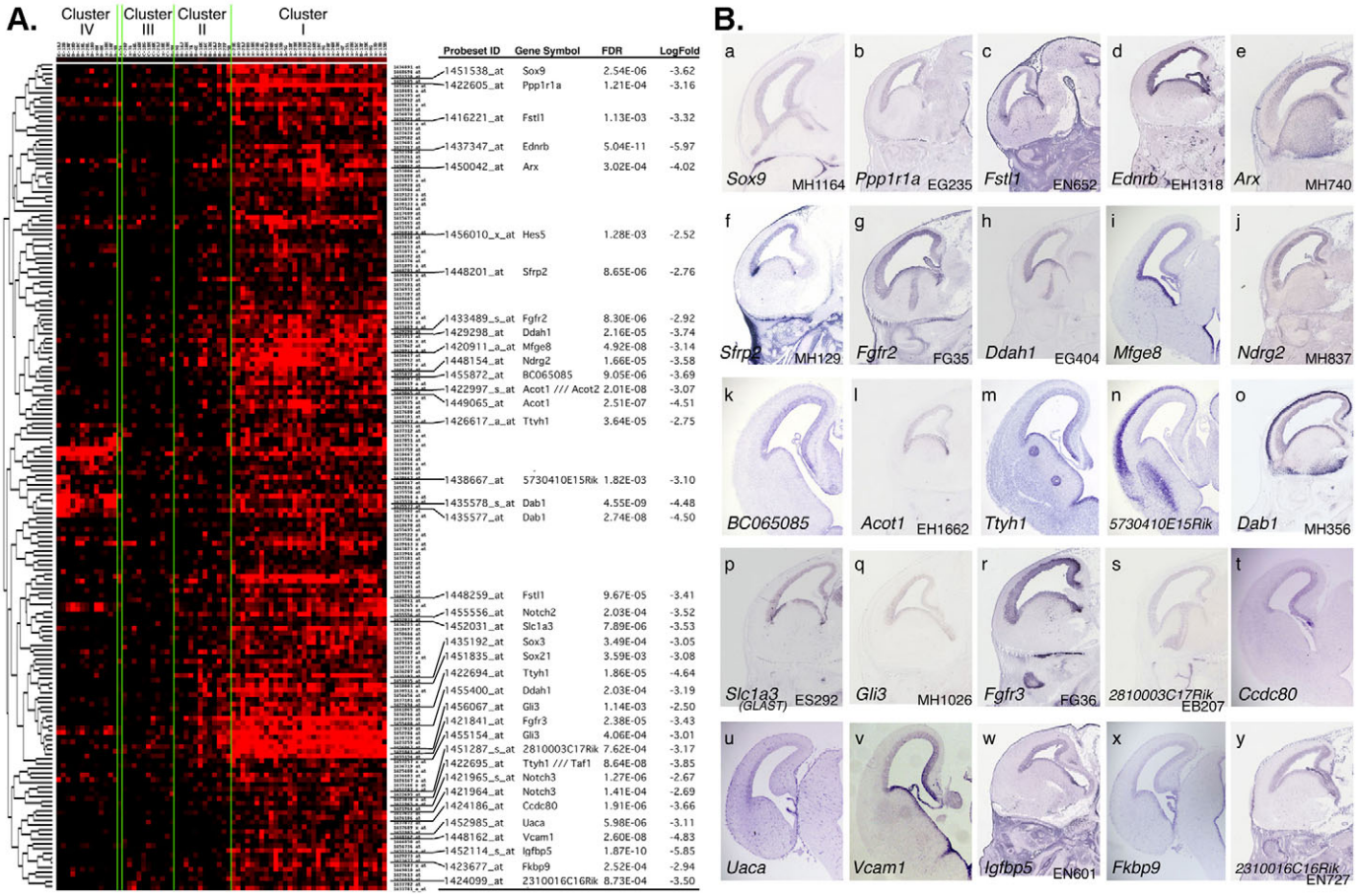

Fig. 4. Expression of Cluster I genes in single-cell cDNAs and in the E14 brain. (**A**) Expression levels of Cluster I genes. Data from the probe sets that were expressed in Cluster I, but not in Cluster II/III, were used for clustering (n=175 probe sets; Welch's t-test, two-tailed, FDR<0.1 log fold-change cut-off <–2.5). Each column indicates one cell, and each row indicates one probe set on the microarray. The expression levels are color-coded from red (high) to black (low). Unlike the Cluster II/III genes (see Fig. 2), no particular pattern was seen in the Cluster I genes, except for the I^+ II^- III^- IV^+ genes (*5730410E15Rik*, *Dab1*). (**B**) Examples of in situ hybridization of the E14 mouse brain for Cluster I genes. In all cases, signals were seen in the VZ. The *5730410E15Rik* and *Dab1* genes were expressed in both the VZ and CP (n,o), consistent with the single-cell gene expression profiles (A). GenePaint set IDs are indicated at the bottom right of some panels.

through the VZ into the SVZ. Thus, our results raise the possibility that the Cluster II cells are the young basal progenitor cells that are migrating through the VZ on their way to the SVZ (see below).

In contrast to the Cluster II/III genes, the same clustering analysis of the Cluster I genes failed to identify subpopulations (Fig. 4A). The in situ signals of the Cluster I genes were almost all confined to the VZ (Fig. 4B), with two exceptions, *5730410E15Rik* and *Dab1* (Fig. 4Bn,o), which showed in situ hybridization signals in both the VZ and the CP in accordance with their gene expression profiles (Fig. 4A). Thus, the Cluster I cells most likely represent the apical progenitor cells that undergo interkinetic nuclear movement.

Variable expression of cell-fate determinants in Cluster I cells

In an attempt to find subpopulations of Cluster I cells by different criteria, we tested whether they could be subdivided according to cell-cycle phases. The expression levels of cell-cycle-related genes could coarsely discriminate the cell-cycle stage of some Cluster I cells (see Fig. S3 in the supplementary material), but no correlation was seen with the expression levels of other genes. As an alternative approach, we examined the expression levels of genes that had documented associations with neural progenitor cells (Fig. 5). One remarkable finding was that Cluster I cells showed highly variable expression of some key molecules that affect progeny fates, including *Hes1*, *Hes5*, *Neurog2*, *Ascl1* and *Dll1* (Fig. 5C-E and see Figs S4-S6 in the supplementary material), whereas the levels of the other genes tested were relatively homogeneous among the Cluster I cells irrespective of expression levels (see Figs S4, S5 in the supplementary material). It is unlikely that these cell-to-cell variations simply reflect differences in the cell-cycle phase because such variations in gene expression were observed among samples at similar cell-cycle phases (see Fig. S3 in the supplementary material). In addition, the variations in the expression levels of these genes were not coincident with the global gene expression patterns (Fig. 1). We noted several characteristic relationships among these determinants. First, there was no correlation in the expression levels of *Hes1* and *Hes5*, which are both thought to be downstream of Notch, within the Cluster I cells (see Figs S4-S6 in the supplementary material), whereas their expression levels did correlate when all the cells from Clusters I to VI were compared. Second, *Hes5*, *Neurog2*, *Ascl1* and *Dll1* were expressed at either a high or a low level in individual Cluster I cells (see Figs S4-S6 in the supplementary material). Although this characteristic pattern of gene expression might partly be explained as an artifact of the

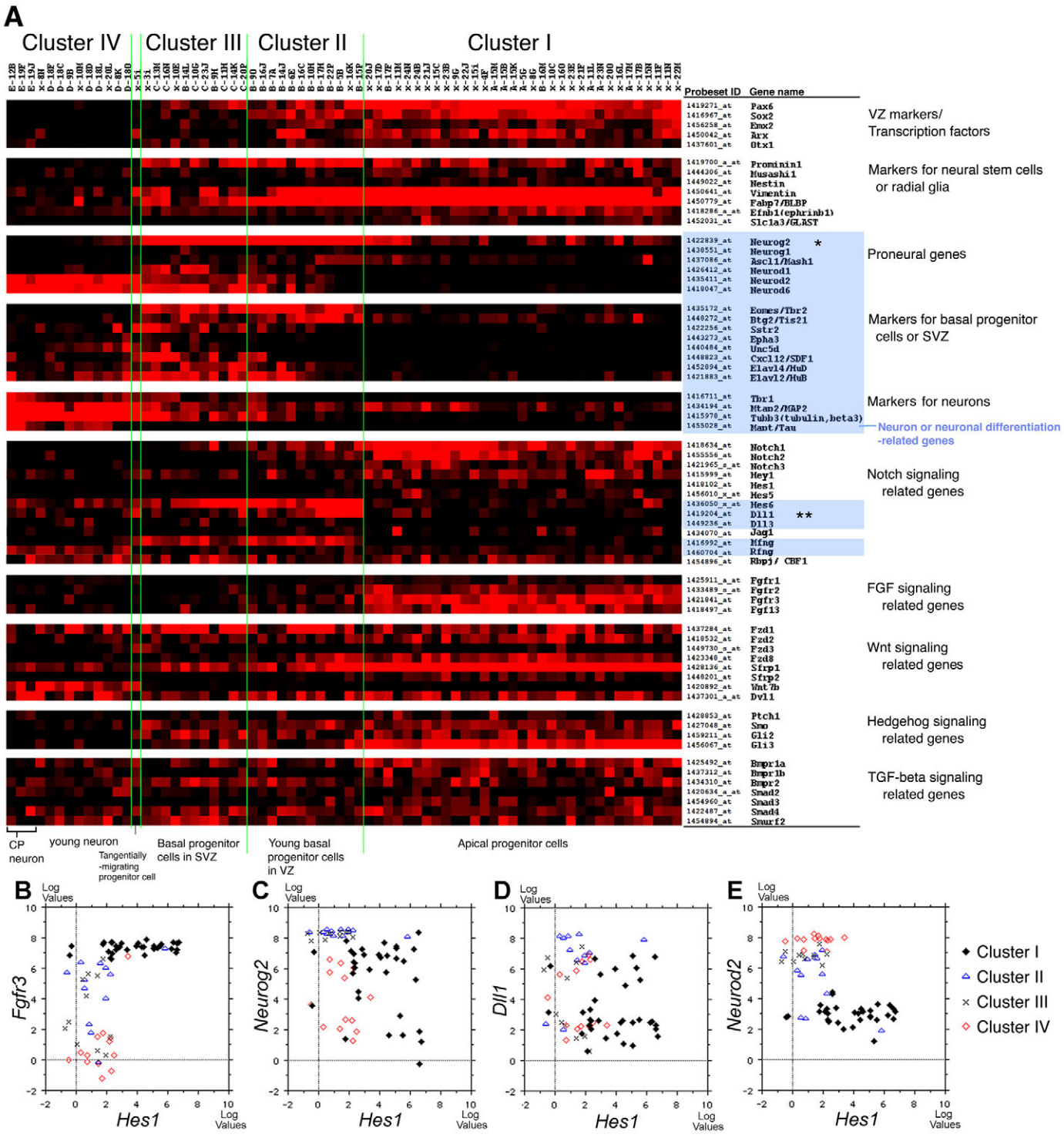

Fig. 5. Expression of marker and signaling pathway genes in single-cell cDNAs, and cell-to-cell variation in the expression of determinants. (**A**) Expression of marker and signaling pathway genes. Each column indicates one cell, and each row indicates one probe set on the microarray. The expression levels are color-coded from red (high) to black (low). All Cluster I cells expressed some neuronal differentiation-related genes at various degrees. *Neurog2* and *Dll1* are marked with asterisks. Cells strongly expressing *Dll1* were mostly Cluster II cells. *Hes3*, *Dll4* and *Jag2* showed low signal levels and are not included in this figure. (**B-E**) Cell-to-cell variations in gene expression in the Cluster I population. Scatter diagram of the *Hes1* and *Fgfr3* (B), *Neurog2* (C), *Dll1* (D) or *Neurod2* (E) expression levels from cDNAs of 70 single cells. Each symbol indicates one cell, and axes are on a natural logarithmic scale.

amplification procedure, the Cluster I cells could nonetheless be separated into four groups according to the combinations of high or low *Hes5*, *Ascl1* and *Dll1* expression (see Fig. S6 in the supplementary material), raising the possibility that the apical progenitors are divided into subgroups by the expression of this subset of genes (see Discussion).

Cluster II cells are committed basal progenitor cells

Our results revealed that the neocortical progenitor cells at this embryonic stage can be categorized into three distinct populations: Cluster I, II and III cells. In particular, the Cluster I and II/III cells differ considerably from each other in their global gene expression profiles, whereas Cluster II and III cells are closely related, even though Cluster II cells are in the VZ and Cluster III cells in the SVZ. We next sought to clarify the lineage relationships among the three cell populations.

Recent studies have shown that Tbr2 (also known as Eomes) is expressed in the basal progenitors as well as in SVZ neurons (Englund et al., 2005). Since this gene is one of the markers that reliably distinguishes Clusters I and II among the VZ progenitor cells, we used Tbr2 to follow the lineage of the Cluster II cells in the VZ. By BrdU-labeling experiments, we found that Tbr2 expression is specific to the G1 phase in VZ progenitor cells, and that at least some of them start to express Tbr2 in early G1 phase (see Fig. S7 in the supplementary material). Furthermore, the expression pattern of a stable EGFP marker driven by the *Tbr2* promoter (Kwon and Hadjantonakis, 2007) strongly suggested that once the cells express EGFP, they never return to the apical surface (see Fig. S7 in the supplementary material). This implies that the Cluster II cells in the VZ do not revert to Cluster I (apical progenitor) cells. We therefore infer that the Cluster II cells are young basal progenitor cells that have 'been committed'. This commitment and the concurrent global change in gene expression from Cluster I to Cluster II occur during or before the early G1 phase.

Nascent basal progenitor cells are a major source of Delta signals

To investigate the mechanisms by which basal (including young basal) progenitor cells are generated from the apical progenitor cells, we analyzed components of canonical signaling pathways that were differentially expressed between Cluster I and Cluster II/III cells, using Ingenuity Pathway Analysis (IPA). The Notch signaling pathway was the most significantly different (P=0.0002 by IPA); among 37 Notch signaling genes in this database, nine (*Dll1*, *Dll3*, *Dtx3*, *Hes5*, *Hey1*, *Mfng*, *Notch1*, *Notch2* and *Notch3*) were included among the 1440 significantly different genes. Although Notch signaling is known to be essential for the maintenance of apical progenitor cells, there has been no detailed analysis at the single-cell level. In Fig. 5A, we summarize the expression of genes of several signaling pathways, including Notch signaling, in single-cell cDNAs. Our gene profiles indicated that the cells strongly expressing *Dll1* were mostly Cluster II cells (Fig. 5A,D). In situ hybridization of *Dll1* indicated a zonal expression pattern, which was strongest in the region 20-40 μm away from the apical surface (Fig. 6A,A′), corresponding to that of some Cluster II/III genes (Fig. 3Aa,b,f,g,n,o). This in situ pattern was consistent with the gene profiles (Fig. 5A) and the anti-Dll1 immunoreactivity seen in the apical half of the VZ (Fig. 6C).

Our findings suggested that young basal progenitor cells are a major source of the Delta signal in vivo, in addition to newborn neurons as previously suggested (Campos et al., 2001). It has been reported that cells in the E14 cerebral wall that are positive for *Dll1* mRNA do not incorporate BrdU and are negative for anti-phosphohistone H3 (PH3), a marker for M-phase cells (Campos et al., 2001). This is consistent with our observation suggesting that the *Dll1*-expressing Cluster II cells were in G1 phase. By contrast, *Dll3* was expressed mainly in the ventral forebrain and weakly in the SVZ of the dorsomedial forebrain (Fig. 6B).

Loss of Notch signaling converts apical progenitor cells to basal progenitor cells via the transient Cluster II state

We next examined the role of Notch signaling in the Cluster I cells directly, by reducing Notch activity with DAPT, a pharmacological inhibitor of γ-secretase (Breunig et al., 2007; Dovey et al., 2001; Nelson et al., 2007). First, we examined the effect of DAPT on E14 cerebral slice cultures. A 20-hour DAPT treatment did not significantly alter the position or number of $Ki67^+$ (a marker for proliferative cells) cells, but dramatically increased both the ratio of $Tbr2^+$ cells in the $Ki67^+$ progenitor cells (Fig. 6D,E,J) and the frequency of non-surface $PH3^+$ dividing cells (Fig. 6F,G,K). Vcam1 was specific for the Cluster I cells in the gene profiles (Fig. 4) and was restricted to the VZ. Vcam1 immunoreactivity was diminished by DAPT treatment (Fig. 6H,I). Very similar observations were made in cells in monolayer-culture, in which most of the DAPT-treated progenitor cells underwent terminal mitosis (see Fig. S8 in the supplementary material).

We next examined the temporal changes in gene expression that distinguished Clusters II and III: *Dll1* was most strongly expressed in Cluster II; *Gadd45g* showed stronger expression in Cluster II than III; and *Svet1* and *Sstr2* were expressed in Cluster III (Figs 2, 3). Treating the slices with DAPT for 7 hours dramatically increased *Dll1* and *Gadd45g* mRNA expression, as compared with the DMSO control (n=7 slices for each) (Fig. 6L,M). In the 20-hour DAPT-treated slices, this increase in *Dll1* expression was not observed, and the *Gadd45g* expression was weakened (n=6 for DMSO, n=5 for DAPT) (Fig. 6N,O). By contrast, no alteration in the *Svet1* or *Sstr2* expression domain was observed in the 7-hour DAPT-treated slices, but their expression did expand in the 20-hour DAPT-treated slices as compared with the control (Fig. 6L-O). These temporal changes in gene expression are very similar to those we observed in progenitor cells in vivo.

Collectively, these results suggest that the elimination of Notch activity converted the apical progenitor cells to basal progenitor cells via the transient Cluster II state.

DISCUSSION

Progenitor subclasses defined by global gene expression patterns

Our gene profiling studies of many single cells (57 progenitor cells and 13 neurons) indicate that the VZ of the mouse E14 cerebrum has only two major subclasses of progenitors, which have distinct global gene expression patterns. One corresponds to the self-renewable apical progenitor cells (Cluster I). The other consists of nascent basal progenitor cells (Cluster II); these cells are in a transient state in the course of differentiating into the SVZ basal progenitor cells (Cluster III). The nascent basal progenitor cells express Dll1, and act to inhibit the differentiation of their neighboring cells, maintaining the population of apical progenitor cells. The two progenitor populations thus constitute a negative-feedback loop, which helps to balance the population of apical progenitor cells and to control the rate of neuronal production (Fig. 6P). This is a mechanism of the type termed 'lateral inhibition' (Artavanis-Tsakonas et al., 1995). We also found that cells of the apical progenitor cell population exhibit significant variations in the expression level of the downstream components of the Notch signal.

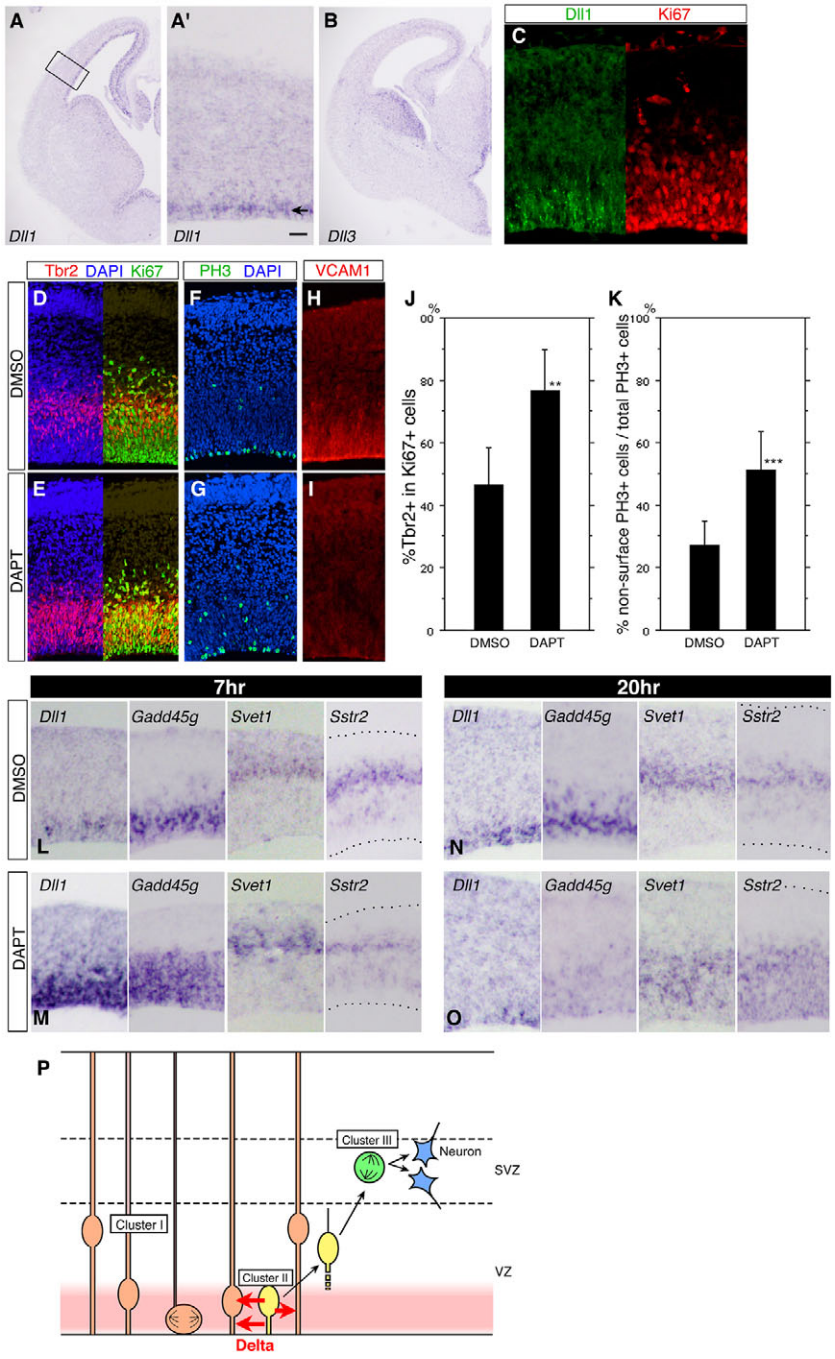

Fig. 6. Delta expression and effect of a Notch signaling inhibitor. (**A**,**A**′) *Dll1* mRNA expression in the E14 mouse brain. (A′) Magnified view of boxed region from A. Signals were most intense in the part of the VZ 20-40 μm away from the apical surface (arrow). Scale bar: 50 μm. (**B**) *Dll3* mRNA expression in the E14 mouse brain. (**C**) Anti-Dll1 (green) and anti-Ki67 (red) immunostaining of the E14 cerebral wall. (**D-K**) Effect of Notch inhibitor in E14 cerebral slice culture. DMSO vehicle (D,F,H) or 10 μM DAPT (E,G,I) was present in the medium for 20 hours. (D,E) Anti-Tbr2 (red), anti-Ki67 (green) and DAPI (blue) staining. (F,G) Anti-PH3 (green) and DAPI (blue) staining. (H,I) Anti-Vcam1 (red) staining. Vcam1 immunoreactivity was diminished by the DAPT treatment (n=7 slices for DMSO, n=8 slices for DAPT). (J) The percentage of Tbr2$^+$ cells amongst Ki67$^+$ cells was significantly increased by DAPT treatment (Mann-Whitney test, two-tailed, $^{**}P$=0.0022, n=8 slices for DAPT and n=7 slices for DMSO). (K) The frequency of non-surface PH3$^+$ cells among total PH3$^+$ cells was significantly increased by DAPT treatment (Mann-Whitney test, two-tailed, $^{***}P$=0.0002, n=8 slices for DAPT and n=11 slices for DMSO). Error bars indicate s.d. The number of apoptotic cells in the VZ was not increased by DAPT treatment compared with the DMSO control, as determined by anti-cleaved caspase 3 immunoreactivity (not shown). (**L-O**) Time-course changes in gene expression in slice culture treated with DMSO (L,N) or DAPT (M,O). In situ hybridization for *Dll1*, *Gadd45g*, *Svet1* or *Sstr2* was performed on samples treated for 7 (L,M) or 20 (N,O) hours. (**P**) Delta-Notch signaling and differentiation of progenitor cells. Cluster I cells are apical progenitor cells, Cluster II cells are nascent basal progenitor cells in the VZ, and Cluster III cells are basal progenitor cells in the SVZ. Cluster II cells (and probably young neurons) express Delta only transiently in the apical half of the VZ, and maintain neighboring Cluster I cells in the undifferentiated state. The choice of the Cluster II cell fate by a daughter cell occurs before and/or during early G1 phase, and the attenuation of Notch signaling presumably triggers this step. During migration to the SVZ, Cluster II cells lose their apical process and become unable to receive a strong Delta signal.

In the single-cell cDNA samples, we failed to identify very young neurons in the VZ. mRNA expression alone might be insufficient to distinguish the very early young neurons (in the G0 state) from the young basal progenitor cells (in early G1 phase). If this is the case, some Cluster II cells might differentiate directly into neurons without division.

Signals regulating the diversification of neural progenitor populations

We demonstrated that Notch signaling is crucial for the conversion between the two progenitor populations (Cluster I versus Cluster II/III). Although Notch signaling is known to be crucial for neurogenesis, to date few studies have focused on its role in progenitor diversification (Breunig et al., 2007; Grandbarbe et al., 2003; Yun et al., 2002). A recent paper, using EGFP as reporter for Cbf1 (Rbpj)-dependent Notch signal transduction, has reported an inheritable difference in Notch signal transduction between two progenitor populations (EGFP-high and EGFP-low or -negative) (Mizutani et al., 2007). The ‘intermediate progenitor cells’ defined by EGFP-low/negative expression appear similar to our Cluster II cells in their low level of expression of *Hes1*, *Hes5*, *Notch1-3* and *Slc1a3* (*Glast*), and also in their commitment to the neuronal fate. However, there are also clear differences between the EGFP-low/negative progenitors and our Cluster II cells. First, as Cluster II/III cells undergo terminal mitosis, their progenitor state is transient and cannot therefore be inherited by the daughter cells. Thus, the heritable difference proposed in the study (Mizutani et al., 2007) does not necessarily coincide with the difference between Clusters

I and II/III. Second, because of the variable expression levels that we saw in Cluster I cells, these cells might include both subpopulations of the Notch transduction state described by Mizutani et al. If this is the case, the differential expression we observed for the cell-fate determinants (*Hes1*, *Hes5* and Notch receptors) in these cells (Fig. 5 and see Figs S4, S5 in the supplementary material) must be partly heritable. Third, we did not detect any difference in the Cbf1 expression level between Cluster I and Cluster II/III cells, but found a similar degree of variation in its expression level within both Cluster I and Cluster II/III cells (see Figs S4, S5 in the supplementary material). Therefore, the low- and high-level Cbf1-EGFP-expressing cells do not seem to correlate with the Cluster I and II/III populations, and might instead contain a mixed population of Cluster I and Cluster II/III cells at different ratios, i.e. the different levels of Cbf1-EGFP expression might reflect a mixture of cells of different states of neuronal commitment. Global gene expression profiling of individual EGFP-high cells and EGFP-low/negative cells will distinguish among these possibilities.

We identified many genes that were differentially expressed between the apical progenitor (Cluster I) cells and the basal progenitor (Cluster II/III) cells. Some of these are involved in canonical signaling pathways other than Notch, such as the FGF and Hedgehog pathways, consistent with the findings of previous studies (de la Pompa et al., 1997; Guillemot, 2005; Lien et al., 2006; Vaccarino et al., 1999). Fig. 5A shows the expression levels of all the FGF genes and FGF receptors included in the Over-20 copies probe sets. *Fgfr2* and *Fgfr3* were strongly expressed in the apical progenitor cells (see also Fig. 4Bg,r and Fig. 5B). It is known that JAK-Stat3 signaling acts downstream of Fgf2 to maintain neural progenitor cells, and that Stat3 directly regulates the expression of Dll1 (Yoshimatsu et al., 2006). Our gene profiles further support the notion that cross-talk among these signaling pathways and Notch signaling plays a role in the diversification of progenitor cells.

Delta-Notch signaling: place and timing

Taking into account anti-Dll1 immunoreactivity (Fig. 6C), in situ hybridization signal for *Dll1* (Fig. 6A,A′) and gene profiling data (Fig. 5A), we conclude that the nascent basal progenitor cells [probably in addition to the young neurons in the VZ, which form directly from the apical progenitor cells (Campos et al., 2001)] only transiently activate the Notch pathway in neighboring cells through Dll1 expressed on their surface, on the apical side of the VZ in the cerebral cortex (Fig. 6P). Previous studies have not detected such Dll1 expression in progenitor subpopulations (Mizutani et al., 2007), probably because this Dll1 activity is highly transient. As previously revealed in slice culture (Konno et al., 2008; Miyata et al., 2004), the basal progenitors (and young neurons) retain their apical process for a short period just after birth at the apical surface, and then lose it to exit the VZ. This observation, and the presence of high levels of Dll1 signal in the apical half of the VZ, led us to reasonably assert that the apical process is a major subcellular structure that receives the Dll1 signal. If this is the case, a subsequent retraction of the apical process by basal progenitors will result in the exclusion of these cells from receiving Delta signaling, and force them into an irreversible state of differentiation in vivo.

Fate choice of the daughters of apical progenitors

The apical progenitor cells undergo heterogeneous division (Guillemot, 2005; Huttner and Kosodo, 2005) although they are homogeneous regarding global gene expression. It is, therefore, unlikely that the apical progenitors with a distinct pattern of global gene expression generate a particular combination of daughter cells. Because the nascent basal progenitor cells that express Cluster II genes, such as *Dll1*, *Gadd45g* and *Hes6*, were observed near the apical surface, we infer that selection of the basal progenitor cell fate by daughter cells occurs within a narrow time window (of several hours) during or after the apical division.

Our DAPT experiments suggest that the attenuation of Notch signaling triggers the differentiation of the apical progenitor cells into basal progenitor cells. There are several factors that might affect the Notch signaling level in the daughter cells within such a narrow time window. One is the environment surrounding the cells (including the existence of Dll1-expressing cells) and another is molecular and/or structural differences between the pair of daughter cells, which are intrinsically created by division; this includes the asymmetric segregation of Notch-related molecules, such as Numb (Shen et al., 2002; Zhong et al., 1996), and/or morphological asymmetry of the daughter cell pair depending on the inheritance of the basal radial process (Buchman and Tsai, 2007; Fishell and Kriegstein, 2003; Miyata et al., 2004). Intercellular variations in the expression level of determinants might be an additional factor. As we observed, the apical progenitor cells have intercellular variations in the level of downstream determinants of Notch. If such variations exist in the dividing apical progenitor cells, they will be inherited by the daughter cells and are likely to bias their fate choice.

Variations in Notch signaling components among the Cluster I population

Fluctuation in the expression levels of cell-fate determinants downstream of Notch (e.g. *Hes1*, *Hes5* and *Neurog2*) appeared specific to Cluster I cells (Fig. 5C and see Figs S4, S5 in the supplementary material). Although this finding might partly result from measurement errors owing to low levels of mRNAs, it is more likely that the observed variations reflect real fluctuations in the expression levels of these genes, as our amplification for mRNAs is reliable (see Fig. S2 in the supplementary material) (Kurimoto et al., 2006; Kurimoto et al., 2007) and the probe sets for *Neurog2*, *Hes1* and *Hes5* function well enough to detect differences among the clusters (Fig. 5C and see Figs S4, S5 in the supplementary material). This variation does not correlate with global gene expression patterns that reflect the differentiation versus non-differentiation tendency, implying that the variations among these Cluster I cells are not equivalent to the differences between the Cluster I and Cluster II cells. This fluctuation in gene expression might occur within a single cell over time in vivo, due to transient contacts with surrounding Dll1 sources and/or oscillatory gene expression. Indeed, a recent real-time imaging study revealed that the expression levels of *Hes1* and *Neurog2* (and *Dll1*) oscillate in complementary phases in neural progenitor cells (Shimojo et al., 2008). One inconsistency is that our analysis of the Cluster I cells did not show a clear negative correlation between *Hes1* and *Neurog2* (Fig. 5C) unless the Cluster II/III cells were included. This discrepancy might arise from a difference or delay in phase between transcription and translation.

Alternatively, this variation might reflect an actual diversity among the Cluster I cells. We found that the Cluster I cells could be segregated into four discrete groups according to the expression levels of *Hes5*, *Ascl1* and *Dll1* (see Fig. S6 in the supplementary material). Because of the low-to-intermediate expression levels of these genes and owing to the limited number of individual Cluster I cells, we cannot accurately assess the contribution of measurement errors. Nonetheless, the overall expression levels of these three genes in Cluster I cells appeared to be virtually independent of the *Hes1* and *Neurog2* expression levels, prompting us to speculate that there are subgroups among the apical progenitors that are defined by

the differential expression of a limited number of genes. To fully understand the significance of this diversity, it will be important to establish whether the differential expression of these genes in Cluster I cells is inherited by the daughter cells or is merely transient. Time-lapse analyses of GFP-reporter constructs will be useful in addressing this issue. Investigation of these mechanisms will help to elucidate how progenitor divisions are controlled to generate the appropriate numbers and types of daughter cells at the correct time.

We thank Mr Kenichiro Uno and Ms Junko Nishio for their excellent help with the microarray experiments and Dr Takaki Miyata (Nagoya University) and Dr Magdalena Götz (GSF-Institute of Stem Cell Research, Neuherberg, Germany) for valuable discussion. This work was supported in part by a CREST from the Japan Science and Technology Agency (F.M.) and by grant KAKENHI (15700264, 18680030) from the Ministry of Education, Culture, Sports, Science and Technology of Japan (A.K.).

Supplementary material

Supplementary material for this article is available at http://dev.biologists.org/cgi/content/full/135/18/3113/DC1

References

Artavanis-Tsakonas, S., Matsuno, K. and Fortini, M. E. (1995). Notch signaling. *Science* **268**, 225-232.

Breunig, J. J., Silbereis, J., Vaccarino, F. M., Sestan, N. and Rakic, P. (2007). Notch regulates cell fate and dendrite morphology of newborn neurons in the postnatal dentate gyrus. *Proc. Natl. Acad. Sci. USA* **104**, 20558-20563.

Britz, O., Mattar, P., Nguyen, L., Langevin, L. M., Zimmer, C., Alam, S., Guillemot, F. and Schuurmans, C. (2006). A role for proneural genes in the maturation of cortical progenitor cells. *Cereb. Cortex* **16 Suppl. 1**, i138-i151.

Buchman, J. J. and Tsai, L. H. (2007). Spindle regulation in neural precursors of flies and mammals. *Nat. Rev. Neurosci.* **8**, 89-100.

Campos, L. S., Duarte, A. J., Branco, T. and Henrique, D. (2001). mDll1 and mDll3 expression in the developing mouse brain: role in the establishment of the early cortex. *J. Neurosci. Res.* **64**, 590-598.

Chenn, A. and McConnell, S. K. (1995). Cleavage orientation and the asymmetric inheritance of Notch1 immunoreactivity in mammalian neurogenesis. *Cell* **82**, 631-641.

de la Pompa, J. L., Wakeham, A., Correia, K. M., Samper, E., Brown, S., Aguilera, R. J., Nakano, T., Honjo, T., Mak, T. W., Rossant, J. et al. (1997). Conservation of the Notch signalling pathway in mammalian neurogenesis. *Development* **124**, 1139-1148.

Dovey, H. F., John, V., Anderson, J. P., Chen, L. Z., de Saint Andrieu, P., Fang, L. Y., Freedman, S. B., Folmer, B., Goldbach, E., Holsztynska, E. J. et al. (2001). Functional gamma-secretase inhibitors reduce beta-amyloid peptide levels in brain. *J. Neurochem.* **76**, 173-181.

Englund, C., Fink, A., Lau, C., Pham, D., Daza, R. A., Bulfone, A., Kowalczyk, T. and Hevner, R. F. (2005). Pax6, Tbr2, and Tbr1 are expressed sequentially by radial glia, intermediate progenitor cells, and postmitotic neurons in developing neocortex. *J. Neurosci.* **25**, 247-251.

Fishell, G. and Kriegstein, A. R. (2003). Neurons from radial glia: the consequences of asymmetric inheritance. *Curr. Opin. Neurobiol.* **13**, 34-41.

Gal, J. S., Morozov, Y. M., Ayoub, A. E., Chatterjee, M., Rakic, P. and Haydar, T. F. (2006). Molecular and morphological heterogeneity of neural precursors in the mouse neocortical proliferative zones. *J. Neurosci.* **26**, 1045-1056.

Götz, M. and Huttner, W. B. (2005). The cell biology of neurogenesis. *Nat. Rev. Mol. Cell Biol.* **6**, 777-788.

Grandbarbe, L., Bouissac, J., Rand, M., Hrabe de Angelis, M., Artavanis-Tsakonas, S. and Mohier, E. (2003). Delta-Notch signaling controls the generation of neurons/glia from neural stem cells in a stepwise process. *Development* **130**, 1391-1402.

Guillemot, F. (2005). Cellular and molecular control of neurogenesis in the mammalian telencephalon. *Curr. Opin. Cell Biol.* **17**, 639-647.

Hartfuss, E., Galli, R., Heins, N. and Gotz, M. (2001). Characterization of CNS precursor subtypes and radial glia. *Dev. Biol.* **229**, 15-30.

Haubensak, W., Attardo, A., Denk, W. and Huttner, W. B. (2004). Neurons arise in the basal neuroepithelium of the early mammalian telencephalon: a major site of neurogenesis. *Proc. Natl. Acad. Sci. USA* **101**, 3196-3201.

Huttner, W. B. and Kosodo, Y. (2005). Symmetric versus asymmetric cell division during neurogenesis in the developing vertebrate central nervous system. *Curr. Opin. Cell Biol.* **17**, 648-657.

Konno, D., Shioi, G., Shitamukai, A., Mori, A., Kiyonari, H., Miyata, T. and Matsuzaki, F. (2008). Neuroepithelial progenitors undergo LGN-dependent planar divisions to maintain self-renewability during mammalian neurogenesis. *Nat. Cell Biol.* **10**, 93-101.

Kriegstein, A., Noctor, S. and Martinez-Cerdeno, V. (2006). Patterns of neural stem and progenitor cell division may underlie evolutionary cortical expansion. *Nat. Rev. Neurosci.* **7**, 883-890.

Kurimoto, K., Yabuta, Y., Ohinata, Y., Ono, Y., Uno, K. D., Yamada, R. G., Ueda, H. R. and Saitou, M. (2006). An improved single-cell cDNA amplification method for efficient high-density oligonucleotide microarray analysis. *Nucleic Acids Res.* **34**, e42.

Kurimoto, K., Yabuta, Y., Ohinata, Y. and Saitou, M. (2007). Global single-cell cDNA amplification to provide a template for representative high-density oligonucleotide microarray analysis. *Nat. Protoc.* **2**, 739-752.

Kwon, G. S. and Hadjantonakis, A. K. (2007). Eomes::GFP-a tool for live imaging cells of the trophoblast, primitive streak, and telencephalon in the mouse embryo. *Genesis* **45**, 208-217.

Lien, W. H., Klezovitch, O., Fernandez, T. E., Delrow, J. and Vasioukhin, V. (2006). alphaE-catenin controls cerebral cortical size by regulating the hedgehog signaling pathway. *Science* **311**, 1609-1612.

Miyata, T., Kawaguchi, A., Saito, K., Kawano, M., Muto, T. and Ogawa, M. (2004). Asymmetric production of surface-dividing and non-surface-dividing cortical progenitor cells. *Development* **131**, 3133-3145.

Mizutani, K. I., Yoon, K., Dang, L., Tokunaga, A. and Gaiano, N. (2007). Differential Notch signalling distinguishes neural stem cells from intermediate progenitors. *Nature* **449**, 351-355.

Nelson, B. R., Hartman, B. H., Georgi, S. A., Lan, M. S. and Reh, T. A. (2007). Transient inactivation of Notch signaling synchronizes differentiation of neural progenitor cells. *Dev. Biol.* **304**, 479-498.

Noctor, S. C., Martinez-Cerdeno, V., Ivic, L. and Kriegstein, A. R. (2004). Cortical neurons arise in symmetric and asymmetric division zones and migrate through specific phases. *Nat. Neurosci.* **7**, 136-144.

Sauer, M. E. and Walker, B. E. (1959). Radioautographic study of interkinetic nuclear migration in the neural tube. *Proc. Soc. Exp. Biol. Med.* **101**, 557-560.

Shen, Q., Zhong, W., Jan, Y. N. and Temple, S. (2002). Asymmetric Numb distribution is critical for asymmetric cell division of mouse cerebral cortical stem cells and neuroblasts. *Development* **129**, 4843-4853.

Shimojo, H., Ohtsuka, T. and Kageyama, R. (2008). Oscillations in notch signaling regulate maintenance of neural progenitors. *Neuron* **58**, 52-64.

Suzuki, R. and Shimodaira, H. (2006). Pvclust: an R package for assessing the uncertainty in hierarchical clustering. *Bioinformatics* **22**, 1540-1542.

Takahashi, T., Nowakowski, R. S. and Caviness, V. S., Jr (1995). The cell cycle of the pseudostratified ventricular epithelium of the embryonic murine cerebral wall. *J. Neurosci.* **15**, 6046-6057.

Tarabykin, V., Stoykova, A., Usman, N. and Gruss, P. (2001). Cortical upper layer neurons derive from the subventricular zone as indicated by Svet1 gene expression. *Development* **128**, 1983-1993.

Tietjen, I., Rihel, J. M., Cao, Y., Koentges, G., Zakhary, L. and Dulac, C. (2003). Single-cell transcriptional analysis of neuronal progenitors. *Neuron* **38**, 161-175.

Vaccarino, F. M., Schwartz, M. L., Raballo, R., Nilsen, J., Rhee, J., Zhou, M., Doetschman, T., Coffin, J. D., Wyland, J. J. and Hung, Y. T. (1999). Changes in cerebral cortex size are governed by fibroblast growth factor during embryogenesis. *Nat. Neurosci.* **2**, 246-253.

Yoon, K. and Gaiano, N. (2005). Notch signaling in the mammalian central nervous system: insights from mouse mutants. *Nat. Neurosci.* **8**, 709-715.

Yoshimatsu, T., Kawaguchi, D., Oishi, K., Takeda, K., Akira, S., Masuyama, N. and Gotoh, Y. (2006). Non-cell-autonomous action of STAT3 in maintenance of neural precursor cells in the mouse neocortex. *Development* **133**, 2553-2563.

Yun, K., Fischman, S., Johnson, J., Hrabe de Angelis, M., Weinmaster, G. and Rubenstein, J. L. (2002). Modulation of the notch signaling by Mash1 and Dlx1/2 regulates sequential specification and differentiation of progenitor cell types in the subcortical telencephalon. *Development* **129**, 5029-5040.

Zhong, W., Feder, J. N., Jiang, M. M., Jan, L. Y. and Jan, Y. N. (1996). Asymmetric localization of a mammalian numb homolog during mouse cortical neurogenesis. *Neuron* **17**, 43-53.